

# Phenomenological Dynamical Mean-Field Theory of Temperature-Dependent

*by* Wiwik Dahani

---

**Submission date:** 03-May-2026 12:28AM (UTC+0700)

**Submission ID:** 2449972008

**File name:** Paper\_Makara\_UI\_Listiana.pdf (619.16K)

**Word count:** 4638

**Character count:** 24164

## Phenomenological Dynamical Mean-Field Theory of Temperature-Dependent Optical Conductivity and Metal-Insulator Transition in $\text{La}_{0.7}\text{Ca}_{0.3}\text{MnO}_3$

Listiana Satiawati<sup>1,2\*</sup>, Adam BCahaya<sup>1</sup>, Eddwi H. Hasdeo<sup>3</sup>, Muhammad Aziz Majidi<sup>1†</sup>,  
Anto Sulaksono<sup>1</sup>, Andriwo Rusydi<sup>4,5,6</sup>

1. Department of Physics, Faculty of Mathematics and Natural Sciences, Universitas Indonesia, Depok 16424, Indonesia
2. Petroleum Engineering Department, Faculty of Earth and Energy Technology, Universitas Trisakti, Jakarta 11440, Indonesia
3. Research Center for Physics, Indonesian Institute of Sciences, Kompleks Puspiptek, Serpong 15314, Indonesia
4. Department of Physics, National University of Singapore, Singapore 117542, Singapore
5. Singapore Synchrotron Light Source, National University of Singapore, Singapore 117542, Singapore
6. NUSNNI-Nanocore National University of Singapore, Singapore 117542, Singapore

\*e-mail: [listianasatiawati@trisakti.ac.id](mailto:listianasatiawati@trisakti.ac.id)  
†e-mail: [azizmajidi@sci.ui.ac.id](mailto:azizmajidi@sci.ui.ac.id)

### Abstract

As an extension of our previous theoretical study, we perform temperature-dependent optical conductivity calculations on  $\text{La}_{0.7}\text{Ca}_{0.3}\text{MnO}_3$  over a wide photon-energy range up to  $\sim 22$  eV, aiming to capture the metal-insulator transition while preserving the general temperature-dependent profile at higher photon energies. The system is modeled with simple Mn-O coordination via the tight-binding method, where some hopping integrals are considered functions of magnetization. Upon incorporating the static Jahn-Teller effect with Coulomb-Hubbard and magnetic exchange interactions, with the exception of a quantitative difference in the calculated  $T_c$  of 160 K versus the experimental value (260 K) and discrepancies in the mid-energy regime, the results reproduce the qualitative temperature-dependent optical conductivity trends, especially for the low- and high-energy regimes, as observed in the experimental data. This qualitative agreement is achieved by setting the magnetization-dependent hopping parameters for the Mn-O hopping parameters,  $t_a$  and  $t_b$ , as  $t_{a(b)} = t_{a(b)}^{(0)} + t_{a(b)}^{(1)}M + t_{a(b)}^{(2)}M^2$ , with  $t_a^{(0)} = 0.958$  eV,  $t_a^{(1)} = 0$  eV,  $t_a^{(2)} = 0.112$  eV,  $t_b^{(0)} = 0.280$  eV,  $t_b^{(1)} = 0$  eV, and  $t_b^{(2)} = 2.080$  eV. The results underscore the importance of correlation effects arising from the interplay of the lattice, charge, and magnetic degrees of freedom in determining the overall profile of the temperature-dependent optical response of manganite, connecting the physics of the high-energy optical response and the transport properties at the dc limit.

**Keywords:** Dynamical mean-field theory,  $\text{La}_{1-x}\text{Ca}_x\text{MnO}_3$ , metal-insulator transition, optical conductivity, spectral weight transfer

### 1. Introduction

Manganite, a group of transition metal oxides, exhibits various exotic phenomena arising from strong correlations among its many degrees of freedom [1, 2, 3, 4]. These correlations manifest in different transport responses, such as multiferroics, charge ordering, and colossal magnetoresistance, depending on geometrical structures. At low Ca doping,  $\text{LaMnO}_3$  converts antiferromagnetic (AFM) insulators into ferromagnetic (FM) metals. This FM metallic phase undergoes a transition to a paramagnetic (PM) insulator as temperature increases.

Understanding the phase transition of such nonstoichiometric systems using first-principles calculations is highly challenging because this approach typically applies only for ground states [5]. Because of the complexity of such systems,

building an effective model is requisite for determining the origin of this phase transition. An oversimplified low-energy Hamiltonian consisting only of Mn orbitals was proposed for microscopically describing the responses of  $\text{La}_{1-x}\text{Ca}_x\text{MnO}_3$  (LCMO) in the static (dc) limit [6, 7]. However, neglecting the higher energy contribution from hybridization of the Mn-d and O-p orbitals might occlude the grand picture, as it assumes no correlation between low- and high-energy regimes. Ca doping enables two dissimilar Mn ions ( $\text{Mn}^{3+}$  and  $\text{Mn}^{4+}$ ) to undergo charge transfer mediated by O ions via the double-exchange (DE) mechanism [8, 9, 10, 11, 12]. The low- and high-energy phenomena are naturally inseparable in this system.

Measurement of the optical conductivity indicates spectral weight transfer from low- to medium- and high-energy regimes when temperature is varied [13]. As temperature increases, the static (dc limit) optical conductivity undergoes a metal-insulator transition (MIT). The change in the spectral weight in the low-energy regime is then balanced by the change in conductivity in the mid- and high-energy regimes, conserving the total spectral weight.

This result suggests that an effective model for  $\text{La}_{1-x}\text{Ca}_x\text{MnO}_3$  should at least include the Mn-O configuration, while the La and Ca bands can be excluded because they may not considerably affect the temperature dependence of the transport and optical responses [14]. One can further reduce the degrees of freedom by assuming strong Hund's coupling, which fixes the occupation of the  $t_{2g}$  subshell of Mn d orbitals in a high-spin configuration. As an effective model, we focus on two  $e_g$  subshells of Mn and three p orbitals of O.

Previously, Majidi et al. [14] solved this effective Hamiltonian for  $\text{La}_{0.7}\text{Ca}_{0.3}\text{MnO}_3$  within dynamical mean-field theory (DMFT) to address the temperature dependence of the optical conductivity. Despite the simplicity of the model, the temperature dependence of the spectral weight agrees well with the experimental data in the mid- and high-energy regimes [13]. Nevertheless, this model is still incomplete as it cannot represent the MIT phenomenon in the dc limit. Despite incorporating static Jahn-Teller (JT) distortion, the model does not treat the dynamics of JT electron-phonon coupling. It was suggested that the MIT arise from competition between the dynamic JT interaction and FM correlation.

We argue that dynamic JT phonons, in competition with the Anderson-Hasegawa DE mechanism, lead to MIT. At high temperatures, JT phonons are abundant, and magnetization is absent. Itinerant electrons are scattered by JT phonons and can be trapped by forming localized polarons, rendering the system insulating. At low temperatures, the number of JT phonons is much lower, while magnetization tends to strengthen Mn-O electron hopping, which in turn increases electron delocalization, resulting in a metallized phase. Rigorous modelling of such a competing mechanism is a challenging task that requires a more sophisticated solution. In this study, we do not present such a treatment; rather, we propose that the unknown detailed microscopic process of competition between the dynamic JT interaction and the DE-driven FM correlation may be viewed phenomenologically as renormalization of the Mn-O hopping parameters as magnetization develops in the system. In this way, the Mn-O hopping parameters become temperature-dependent through magnetization.

In moving from high to low temperatures, FM correlation starts to develop. This increases the probability of hopping via the DE mechanism. Electron hopping between Mn ions via oxygen through the DE mechanism is pronounced if electron spins are aligned, as postulated by Anderson and Hasegawa [9]. The hopping integral is roughly inversely proportional to temperature. Below a certain temperature (i.e., the FM  $T_c$ ), magnetization starts to develop and becomes larger as temperature decreases further to approach zero. In this model, there are two Mn-O hopping parameters. According to the Anderson-Hasegawa picture [9], with decreasing temperature, magnetization increases, and these two hopping parameters should increase. The enhancement of these two hopping parameters eventually increases the electron mobility, which delocalizes electrons previously trapped in polarons, thus promoting the transition of the system from insulating to metallic around  $T_c$ , concomitant with the transition from PM to FM.

Although the MIT scheme driven by competition between the JT electron-phonon interaction and FM correlation has been widely accepted [2], its relation to the high-energy optical response has not attracted much attention from researchers. Here, we highlight the effect of the change in the magnitude of the Mn-O hopping parameters on modifying the band structure and probability of optical transition between electronic levels to some degree. The data further suggest that the optical response would also be modified as temperature changes across the PM-FM transition and inside the FM phase. We argue that this is the reason why the MIT at the dc limit is accompanied by optical spectral weight transfer in higher photon-energy regimes.

How the DE mechanism competes with the dynamic JT electron-phonon interaction is not yet exactly known. To capture this effect phenomenologically, we model the Mn-O hopping parameters as functions of magnetization, whereas magnetization itself depends on temperature. We proceed with calculating the optical conductivity following the

previously developed method [14]. However, we reconsider the detailed expression of the nonperturbed part of the Hamiltonian as well as the functional forms of the Mn–O hopping parameters as functions of magnetization. Within this improved model, the calculations indicate MIT in the dc limit, while preserving the temperature-dependent profile of the optical conductivity in the low- and high-energy regimes, consistent with the experimental data. We acknowledge that the results do not agree well with the experimental data in the mid-energy regime. We address this in the discussion.

## 2. Model and Method

As in the previous study [14], we define the basis set as consisting of Mn and O atomic orbitals only, which we order as follows:  $|\text{Mn } e_g x^2-y^2, \uparrow\rangle$ ,  $|\text{Mn } e_g 3z^2-r^2, \uparrow\rangle$ ,  $|\text{O}_{1p, \uparrow}\rangle$ ,  $|\text{O}_{2p, \uparrow}\rangle$ ,  $|\text{O}_{3p, \uparrow}\rangle$ ,  $|\text{Mn } e_g x^2-y^2, \downarrow\rangle$ ,  $|\text{Mn } e_g 3z^2-r^2, \downarrow\rangle$ ,  $|\text{O}_{1p, \downarrow}\rangle$ ,  $|\text{O}_{2p, \downarrow}\rangle$ , and  $|\text{O}_{3p, \downarrow}\rangle$ . We argue that these are the minimum number of basis orbitals that are strongly correlated, such that they determine the temperature dependence of the optical conductivity of the system. Here, the La band is ignored on the basis of the assumption that it does not notably contribute to the electron dynamics in the energy region of interest. To span the wide energy spectrum without including all the atomic or Wannier orbitals of La atoms, we then adjust the Mn–O hopping parameters in the model accordingly. We argue that in doing so, we include the effective Mn–O hopping parameters that incorporate the effect of the La orbitals. The effect of Ca doping is only considered as adding extra holes to the system. As a further simplification, we assume that only two  $e_g$  orbitals of Mn play a role in the dynamics of the system, leaving the  $t_{2g}$  electrons “frozen” in the high-spin configuration.

Using the aforementioned basis set, the Hamiltonian can be expressed as follows:

$$H = \frac{1}{N} \sum_{\mathbf{k}} \zeta_{\mathbf{k}}^\dagger [H_0(\mathbf{k})] \zeta_{\mathbf{k}} + \sum_{i, \sigma, \sigma'} U n_{a, i, \sigma} n_{b, i, \sigma'} + \sum_i U_a n_{a, i} n_{a, i} + \sum_i U_b n_{b, i} n_{b, i} - \sum_i J_H \mathbf{S}_i \cdot \mathbf{s}_i \quad (1)$$

where  $\zeta_{\mathbf{k}}^\dagger$  ( $\zeta_{\mathbf{k}}$ ) is a row (column) vector for which the elements are the creation (annihilation) operators associated with the basis states;  $U$  and  $U_{a(b)}$  are the Hubbard–Coulomb interactions for inter- and intra-orbitals, respectively, with  $|a\rangle$  and  $|b\rangle$  being associated with  $|\text{Mn } e_g x^2-y^2\rangle$  and  $|\text{Mn } e_g 3z^2-r^2\rangle$ ; and  $J_H$  is Hund’s coupling between the collective spin  $\mathbf{S}_i$  at the  $t_{2g}$  electrons and itinerant spin  $\mathbf{s}_i$  of an  $e_g$  electron at site  $i$ . Summation over index  $i$  spans all Mn sites in the system.

The first term of Eq. (1) is the kinetic or nonperturbed part constructed using the tight-binding method. In the developed model, the Mn ion is surrounded by six O ions as the nearest neighbors. According to the order of the basis states defined previously, applying the tight-binding approximation gives us a  $10 \times 10$  matrix of the kinetic Hamiltonian as follows:

$$[H_0(\mathbf{k})] = \begin{bmatrix} H_0(\mathbf{k})_{\uparrow} & \mathbf{0} \\ \mathbf{0} & H_0(\mathbf{k})_{\downarrow} \end{bmatrix} \quad (2)$$

where  $\mathbf{0}$  is a  $5 \times 5$  zero matrix, and

$$H_0(\mathbf{k})_{\uparrow(\downarrow)} = \begin{bmatrix} E_{JT} & 0 & -2t_a \cos \frac{k_x c}{2} & -2t_a \cos \frac{k_y c}{2} & -2t_a \cos \frac{k_z c}{2} \\ 0 & -E_{JT} & -2t_b \cos \frac{k_x c}{2} & -2t_b \cos \frac{k_y c}{2} & -2t_b \cos \frac{k_z c}{2} \\ -2t_a \cos \frac{k_x c}{2} & -2t_b \cos \frac{k_x c}{2} & E_p & -4t_o \cos \frac{k_x c}{\sqrt{2}} \cos \frac{k_y c}{\sqrt{2}} & -4t_o \cos \frac{k_x c}{\sqrt{2}} \cos \frac{k_z c}{\sqrt{2}} \\ -2t_a \cos \frac{k_y c}{2} & -2t_b \cos \frac{k_y c}{2} & -4t_o \cos \frac{k_x c}{\sqrt{2}} \cos \frac{k_y c}{\sqrt{2}} & E_p & -4t_o \cos \frac{k_x c}{\sqrt{2}} \cos \frac{k_z c}{\sqrt{2}} \\ -2t_a \cos \frac{k_z c}{2} & -2t_b \cos \frac{k_z c}{2} & -4t_o \cos \frac{k_x c}{\sqrt{2}} \cos \frac{k_z c}{\sqrt{2}} & -4t_o \cos \frac{k_y c}{\sqrt{2}} \cos \frac{k_z c}{\sqrt{2}} & E_p \end{bmatrix} \quad (3)$$

where  $c$  and  $\hbar$  are the lattice constant (assuming a cubic lattice),  $\pm E_{JT}$  are the static JT-split  $e_g$  on-site energies,  $E_p$  is the on-site energy of the oxygen p orbitals,  $t_a(t_b)$  is the hopping parameter connecting Mn  $|a\rangle$  ( $|b\rangle$ ) to the O states, and  $t_o$  is the hopping parameter between two O states. The rest of the terms in Eq. (1) are grouped into the interaction part that will be self-consistently treated in the self-energy matrix.

We solve the Hamiltonian in Eq. (1) using self-consistent DMFT [15, 16]. We do not discuss the detailed self-consistent procedure of DMFT implementation for this system, as presented in Ref. [14]. As in the previous study, our main goal is to calculate the temperature-dependent optical conductivity:

$$\sigma_{\alpha\beta}(\omega) = \frac{\pi e^2}{\hbar c} \int d\nu \left( \frac{f(\nu, \mu, T) - f(\nu + \omega, \mu, T)}{\omega} \right) \frac{1}{N} \sum_{\mathbf{k}} \text{Tr} [v_{\alpha}(\mathbf{k})][A(\mathbf{k}, \nu)][v_{\beta}(\mathbf{k})][A(\mathbf{k}, \nu + \omega)] \quad (4)$$

where  $[v_{\alpha}(\mathbf{k})] = \partial[H_{\alpha}(\mathbf{k})]/\partial k_{\alpha}$  is the velocity matrix;  $[A(\mathbf{k}, \nu)] = \frac{[G(\mathbf{k}, \nu + i0^*)] - [G(\mathbf{k}, \nu - i0^*)]}{2\pi i}$  is the spectral function matrix, with  $[G(\mathbf{k}, \nu \pm i0^*)]$  being the corresponding retarded and advanced Green function matrices; and  $f(\nu, \mu, T)$  is the Fermi-Dirac distribution function, with  $T$  being the temperature and  $\mu$  being the chemical potential. We are only interested in the longitudinal conductivity  $\sigma_{\alpha\alpha}(\omega) = \sigma(\omega)$  which is isotropic in this model.

In the present study, our attempt to reproduce the detailed temperature-dependent profile of the optical conductivity, compared to the experimental data, leads us to propose the dependence of the Mn-O hopping parameters  $t_a$  and  $t_b$  as follows:

$$t_{a(b)} = t_{a(b)}^{(0)} + t_{a(b)}^{(1)}M + t_{a(b)}^{(2)}M^2 \quad (5)$$

where  $M$  is the normalized magnetization, assumed to follow a mean-field trend given by  $M = (1 - T/T_c)^{\gamma}$  below  $T_c$  and  $M = 0$  otherwise, with  $\gamma = 0.5$ . The values of coefficients  $t_{a(b)}^{(0)}$ ,  $t_{a(b)}^{(1)}$ , and  $t_{a(b)}^{(2)}$  are to be determined by the best fit of  $\sigma(\omega)$  to the experimental data. In Ref. [14], we also proposed the temperature dependence of the two Mn-O hopping parameters in a similar manner. However, in this study, we reconsider the detailed dependence of those parameters on magnetization to capture the MIT in the dc limit.

### 3. Results and Discussion

As in the previous study [14], we use the following parameter values for the calculation:  $c = 3.3945 \text{ \AA}$ ,  $E_{JT} = 0.5 \text{ eV}$ ,  $E_p = 6.5 \text{ eV}$ ,  $t_o = 0.6 \text{ eV}$ ,  $U = 10 \text{ eV}$ , and  $J_H = 1.5 \text{ eV}$ . The optical conductivity  $\sigma(\omega)$  calculated at several temperatures using Eq. (4) is presented in Fig. 1 and is compared with the experimental data from Ref. [13]. We divide the photon-energy region into low- (below 5.5 eV), mid- (5.5–12 eV), and high-energy (above 12 eV) regimes following the change in the spectral weight (amplitude of  $\sigma(\omega)$ ). In the low- and high-energy regimes, including the dc limit, the results show that  $\sigma(\omega)$  decreases as temperature increases, where the temperature-dependent profiles adequately reproduce the experimental data. In the mid-energy regime, the experimental data show that  $\sigma(\omega)$  increases as temperature increases, indicating spectral weight transfer from the low- and high-energy regimes to the mid-energy regime while conserving the total integrated spectral weight. However, the present results do not accurately capture the temperature-dependent profile of  $\sigma(\omega)$  in the mid-energy regime, suggesting that the conservation of the total integrated spectral weight is not quite satisfied. In this respect, we acknowledge that the developed model may still lack more important components in the kinetic part of the Hamiltonian to produce more relevant details of the band structure.

Considering the dependence of the two Mn-O hopping parameters on magnetization, as given by Eq. (5), the main finding of this study is the disappearance of the Drude structure, indicated by a drop of  $\sigma(\omega)$  in the dc limit, as temperature increases, signifying MIT, as shown in Fig. 1. This is a new finding not observed in the previous study. As shown in Fig. 1, the present model qualitatively captures the trend of the temperature dependence of  $\sigma(\omega)$  in the low- and high-energy regimes as temperature changes across and below  $T_c$ .

To analyze these results, roughly speaking, there are two contributions to  $\sigma(\omega)$  in Eq. (4): 1) the spectral functions  $[A(\mathbf{k}, \nu)]$  and  $[A(\mathbf{k}, \nu + \omega)]$  and 2) the velocity matrices, the latter of which contain elements proportional to the hopping integrals (Eq. (3)). We then argue that the two Mn-O hopping parameters ( $t_a$  and  $t_b$ ) must be temperature-dependent in some way. Furthermore, as we attempt to tune the  $t_a$  and  $t_b$  values to cause the spectral weight of  $\sigma(\omega)$  to increase or decrease in the mid- and high-energy regimes, we find that proper simultaneous tuning of  $t_a$  and  $t_b$  (as stated in Eq. (5)) automatically controls the Drude structure in the low-energy regime. To best reproduce the temperature-dependent profile of the calculated optical conductivity compared to that of the experimental data, we find that the coefficients in Eq. (5) satisfy the following values:  $t_a^{(0)} = 0.958 \text{ eV}$ ,  $t_a^{(1)} = 0 \text{ eV}$ ,  $t_a^{(2)} = 0.112 \text{ eV}$ ,  $t_b^{(0)} = 0.280 \text{ eV}$ ,  $t_b^{(1)} = 0 \text{ eV}$ , and  $t_b^{(2)} = 2.080 \text{ eV}$ . The best fit requires  $t_a^{(1)}$  and  $t_b^{(1)}$  to be zero, indicating that the hopping parameters depend on magnetization

as an even function, consistent with the cosine function expansion of the angle between neighboring Mn spins, as suggested by Anderson and Hasegawa [9].

To analyze the behavior of  $\sigma(\omega)$  in the low-energy regime, including the MIT captured in the dc limit, we display the density of states (DOS) plots in Figs. 2 and 3. As shown in Fig. 2, at high temperatures, the chemical potential,  $\mu$ , lies in the  $e_g^b$  band. Thus, we conclude that this  $e_g^b$  band of Mn is responsible for dc conductivity. This is confirmed by the fact that the dc conductivity value is sensitive to the change in  $t_b$ . Even at high temperatures where the dc conductivity value considerably drops, the DOS does not exhibit a bandgap near  $\mu$ . This indicates that the LCMO PM insulator state has a small finite conductivity value, as confirmed by resistivity measurement reported in Ref. [17]. Here, the term insulator does not necessarily correspond to zero conductivity but indicates relatively high resistivity that tends to further increase as temperature decreases. Likewise, the term metal here indicates a decreasing resistivity trend as temperature decreases [2]. Figure 3 presents a comparison of the spin-up and spin-down components of the DOS for  $T = 194$  K (above  $T_c$ ) and  $T = 30$  K (below  $T_c$ ). At  $T > T_c$ , the PM phase is indicated by the coincidence of the spin-up and down components of the DOS. Here, thermal energy suppresses magnetization to optimize the entropy at equilibrium. In the absence of magnetization, the hopping parameters  $t_a$  and  $t_b$  take their lowest values.

This situation leads to the lowest value of DOS at  $\mu$ , which also implies the lowest value of dc conductivity. In contrast, at low temperatures ( $T < T_c$ ) where the magnetization value is sufficiently large,  $t_a$  and  $t_b$  achieve significantly larger values than their minimum values at high temperatures. The larger value of  $t_b$  plays a key role in delocalizing electrons; hence, the system adequately forms a metallic phase. Optical conductivity in the low-energy regime arises from intraband transition of the lower  $e_g^b$  orbital. The weight of this spectrum mainly depends on the value of  $t_b$ , the hopping parameter. The signature of Drude peak at low temperatures is related to the significant increase in the DOS value at  $\mu$ .

We now analyze the optical conductivity in higher photon-energy regimes. To do this, we present the partial or projected DOS in Fig. 2 to assign each peak in the total DOS. Oxygen bands are located around  $-6$  eV, accounting for  $\sigma(\omega)$  in the mid- and high-energy regimes. The manganese  $e_g^b$  bands are split and are located at low energy due to the static JT effect and  $J_J$  coupling. In comparison, the  $e_g^a$  bands are located at high energy due to the strong on-site interaction  $U$ . In the mid-energy regime, both intraband  $e_g^b$  and interband  $O-e_g^b$  contribute to conductivity. These features should result in peaks that might have been obscured by spectral broadening. Although the features do not exactly match those in Ref. [13], the overall temperature-dependent trends show reasonable agreement. In the high-energy regime, interband  $e_g^b-e_g^a$  and  $O-e_g^a$  transitions take place. The increase in  $\sigma(\omega)$  as temperature decreases across and below  $T_c$  in this energy region arises from the inverse proportionality of  $t_a$  with respect to temperature.

We note that the simplified model is not to be quantitatively compared with the experimental results in terms of the FM transition temperature and the span of three different energy regimes. The calculated  $T_c$  is approximately 160 K, compared to the measured  $T_c = 260$  K. Therefore, in Fig. 1 (inset), we show different sets of temperatures in comparison to the experimental values.

Analysis of the DOS across  $T_c$  indicates the PM-to-FM transition (Fig. 3). At low temperatures, the spin-up (red line) and spin-down (green line) DOS split, yielding a finite magnetization value. Through a self-consistent scheme, this magnetization enhances the hopping parameters and thus increases  $\sigma(\omega)$  in the low- and high-energy regimes. In contrast, the PM state at high temperatures is evident because the DOS of different spins overlay each other (black and blue lines).

Finally, the calculation results deviate from the experimental data in the detailed profile of  $\sigma(\omega)$ , such as in the mid-energy regime. However, we note that this is understandable as the model neglects many other atomic orbitals that possibly contribute to forming the actual band structure of the material in the relevant energy range. Nevertheless, we claim that the developed minimum model successfully captures the essential physics governing the MIT and the wide-energy-range spectral weight transfer phenomenon in  $\text{La}_{0.7}\text{Ca}_{0.3}\text{MnO}_3$ .

#### 4. Conclusions

We formulated an effective model for  $\text{La}_{0.7}\text{Ca}_{0.3}\text{MnO}_3$  to address the temperature-dependent optical conductivity over a wide photon-energy range (0–22 eV), along with the MIT at the dc limit. We solve the developed model within DMFT. We propose that the unknown microscopic process of competition between the JT electron-phonon interaction and the FM correlation can be phenomenologically viewed as renormalization of the Mn–O hopping parameters as a function of magnetization. The dependence of the Mn–O hopping parameters on magnetization plays an important role in the MIT

across the FM  $T_c$  and affects spectral weight transfer between different photon-energy regimes. The reasonable agreement of the calculated temperature-dependent optical conductivity with the experimental data underscores the importance of interplay among the JT electron–phonon interaction, DE mechanism, and Coulomb–Hubbard electron–electron interactions in giving rise to the unique temperature-dependent transport and optical response of manganite.

### Acknowledgements

We acknowledge the funding support from the Ministry of Research, Technology, and Higher Education of the Republic of Indonesia through PDUPT Research Grant No. 374/UN2.R3.1/HKP05.00/2018.

### References

- [1] Jin, S., Tiefel T.H., Mc Cormack, M., Fastnacht, R.A., Ramesh, R., Chen, L.H. 1994. Thousandfold change in resistivity in magnetoresistive La-Ca-Mn-O films. *Science*. 264 413–415 ISSN 0036-8075. (Preprint <https://science.sciencemag.org/content/264/5157/413.full.pdf>). URL <https://science.sciencemag.org/content/264/5157/413>.
- [2] Salamon, M.B., Jaime, M. 2001. The physics of manganites: Structure and transport. *Rev. Mod. Phys.* 73(3) 583–628. URL <https://link.aps.org/doi/10.1103/RevModPhys.73.583>.
- [3] Cheong, S.W., Mostovoy, M. 2007. Multiferroics: a magnetic twist for ferroelectricity. *Nature Materials* 6 13 EP – review Article URL <https://doi.org/10.1038/nmat1804>.
- [4] Saitoh, E., Okamoto, S., Takahashi, K.T., Tobe, K., Yamamoto, K., Kimura, T., et al. 2001. Observation of orbital waves as elementary excitations in a solid. *Nature* 410 180–183 ISSN 1476-4687 URL <https://doi.org/10.1038/35065547>.
- [5] Martin, R.M. 2004. *Electronic structure: basic theory and practical methods*. Cambridge University Press. 5-6-2012.
- [6] Millis, A.J., Mueller, R., Shraiman, B.I. 1996. Fermi-liquid-to-polaron crossover. II. Double exchange and the physics of colossal magnetoresistance. *Phys. Rev. B* 54(8) 5389–5404 URL <https://link.aps.org/doi/10.1103/PhysRevB.54.5389>.
- [7] Ramakrishnan, T.V., Krishnamurthy, H.R., Hassan, S.R., Pai, G.V. 2004. Theory of insulator metal transition and colossal magnetoresistance in doped manganites. *Phys. Rev. Lett.* 92(15) 157203 URL <https://link.aps.org/doi/10.1103/PhysRevLett.92.157203>.
- [8] Moreo, A., Yunoki, S., Dagotto, E. 1999. Phase Separation Scenario for Manganese Oxides and Related Materials. *Science*, 283 2034–2040 ISSN 0036-8075 (Preprint <https://science.sciencemag.org/content/283/5410/2034.full.pdf>) URL <https://science.sciencemag.org/content/283/5410/2034>.
- [9] Anderson, P.W., Hasegawa, H. 1955. Considerations on double exchange. *Phys. Rev.* 100(2) 675–681 URL <https://link.aps.org/doi/10.1103/PhysRev.100.675>.
- [10] Quijada, M., Cerne, J., Simpson, J.R., Drew, H.D., Ahn, K. H., Millis, A.J., et al. 1998. Optical conductivity of manganites: crossover from Jahn-Teller small polaron to coherent transport in the ferromagnetic state. *Phys. Rev. B* 58(24) 16093–16102 URL <https://link.aps.org/doi/10.1103/PhysRevB.58.16093>.
- [11] Amelichev, V.A., Guttler, B., Gorbenco, O.Y., Kaul, A.R., Bosak, A.A., Ganin, A.Y. 2001. Structural and magnetic ordering in  $\text{La}_{0.5}\text{Ca}_{0.5}\text{Ba}_x\text{MnO}_3$  ( $0 \leq x \leq 0.5$ ). *Phys. Rev. B* 63(10) 104430 URL <https://link.aps.org/doi/10.1103/PhysRevB.63.104430>.
- [12] de Gennes, P.G. 1960. Effects of double exchange in magnetic crystals. *Phys. Rev.* 118(1) 141–154. URL <https://link.aps.org/doi/10.1103/PhysRev.118.141>.
- [13] Rusydi, A., Rauer, R., Neuber, G., Bastjan, M., Mahns, I., Miller, S., et al. 2008. Metal-insulator transition in manganites: changes in optical conductivity up to 22 eV. *Phys. Rev. B* 78(2008),125110 78
- [14] Majidi, A., Su, H., Feng, Y.P., Ruebhausen, M., Rusydi, A. 2011. Theory of high-energy optical conductivity and the role of oxygens in manganites. *Phys. Rev. B* 84. 075136.
- [15] Georges, A., Kotliar, G., Krauth, W., Rozenberg, M.J. 1996. Dynamical mean-field theory (DMFT). *Rev. Mod. Phys.* 68(1) 13–125 URL <https://link.aps.org/doi/10.1103/RevModPhys.68.13>.
- [16] Furukawa, N. 1998. Thermodynamics of the double exchange systems. arXiv:cond-mat/9812066 [cond-mat.str-el] (Preprint [cond-mat/9812066](https://arxiv.org/abs/cond-mat/9812066)).
- [17] Ramirez, A.P., Schiffer, P., Cheong, S.W., Chen, C.H., Bao, W., Palstra, T.T.M., et al. 1996. Thermodynamic and electron diffraction signatures of charge and spin ordering in  $\text{La}_{1-x}\text{Ca}_x\text{MnO}_3$ . *Phys. Rev. Lett.* 76(17) 3188–3191 URL <https://link.aps.org/doi/10.1103/PhysRevLett.76.3188>

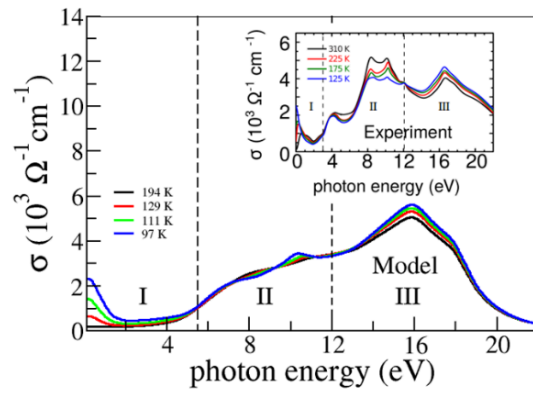


Figure 1: Dynamic optical conductivity  $\sigma$  from Eq. (4) as a function of photon energy at several temperatures. [Inset] Measured optical conductivity from Ref. [13] for comparison. Note that the calculated  $T_c$  of 160 K is smaller than the experimental  $T_c$  of 260 K. Therefore, we show different sets of temperatures across  $T_c$ . Dashed lines indicate the division of low-, mid-, and high-energy regimes.

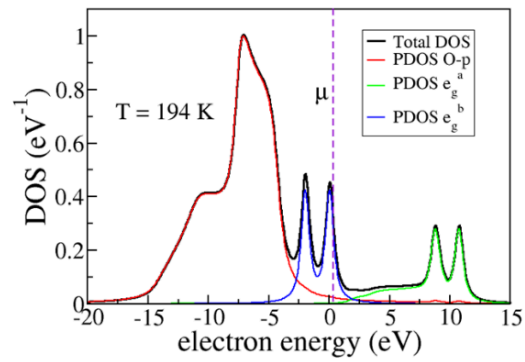


Figure 2: Density of states (DOS) of the  $\text{La}_{0.7}\text{Ca}_{0.3}\text{MnO}_3$  model for  $T=194$  K (above the model  $T_c$ ). Red, blue, and green lines are the projected DOS of oxygen,  $e_g^a$ , and  $e_g^b$  bands, respectively. Vertical dashed lines indicate the position of chemical potential  $\mu$ .

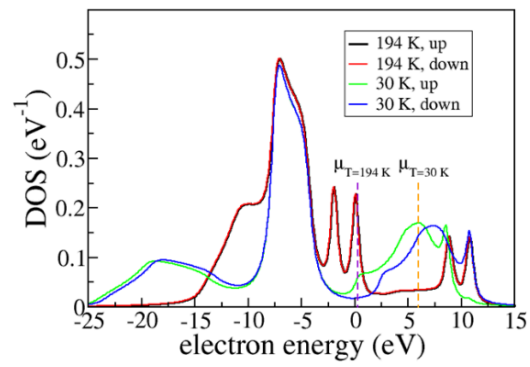


Figure 3: Spin-dependent DOS for two different temperatures. Above  $T_c$ , spin-up (black line) and spin-down (blue line) DOS do not split. Below  $T_c$ , spin-up (red line) and spin-down (green line) DOS split.

# Phenomenological Dynamical Mean-Field Theory of Temperature-Dependent

## ORIGINALITY REPORT

9%

SIMILARITY INDEX

5%

INTERNET SOURCES

8%

PUBLICATIONS

3%

STUDENT PAPERS

## PRIMARY SOURCES

1

[iopscience.iop.org](http://iopscience.iop.org)

Internet Source

2%

2

Submitted to Badan PPSDM Kesehatan  
Kementerian Kesehatan

Student Paper

2%

3

Edoardo Baldini. "Nonequilibrium Dynamics of Collective Excitations in Quantum Materials", Springer Science and Business Media LLC, 2018

Publication

1%

4

Choirun Nisaa Rangkuti, Adam B Cahaya, Anugrah Azhar, Muhammad Aziz Majidi, Andrivo Rusydi. "Manifestation of charge/orbital order and charge transfer in temperature-dependent optical conductivity of single-layered Pr Ca MnO ", Journal of Physics: Condensed Matter, 2019

Publication

1%

5

Muhammad Aziz Majidi, Haibin Su, Yuan Ping Feng, Michael Rübhausen, Andrivo Rusydi. "Theory of high-energy optical conductivity and the role of oxygens in manganites", Physical Review B, 2011

Publication

1%

6

M. A. Majidi, E. Thoeng, P. K. Gogoi, F. Wendt et al. "Temperature-dependent and anisotropic optical response of layered Pr Ca

1%

MnO probed by spectroscopic ellipsometry ",  
Physical Review B, 2013

Publication

---

7 L. Satiawati, M. A. Majidi. "Theoretical formulation of optical conductivity of La<sub>0.7</sub>Ca<sub>0.3</sub>MnO<sub>3</sub> exhibiting paramagnetic insulator - ferromagnetic metal transition", AIP Publishing, 2017

Publication

---

8 [scholarship.rice.edu](http://scholarship.rice.edu) <1 %

Internet Source

---

9 Submitted to University of Hong Kong <1 %

Student Paper

---

10 Asish K. Kundu, Sukanta Barman, Krishnakumar S. R. Menon. " Role of Surface Termination in the Metal-Insulator Transition of V O (0001) Ultrathin Films ", ACS Applied Materials & Interfaces, 2021

Publication

---

Exclude quotes On

Exclude matches < 15 words

Exclude bibliography On

# Phenomenological Dynamical Mean-Field Theory of Temperature-Dependent

---

GRADEMARK REPORT

---

FINAL GRADE

GENERAL COMMENTS

**/0**

---

PAGE 1

---

PAGE 2

---

PAGE 3

---

PAGE 4

---

PAGE 5

---

PAGE 6

---

PAGE 7

---

PAGE 8

---